Sustainable Energy & Fuels

ROYAL SOCIETY OF CHEMISTRY

PAPER

View Article Online
View Journal | View Issue

Cite this: *Sustainable Energy Fuels*, 2023, 7, 5283

Predicting the physical properties of three-component lignocellulose derived advanced biofuel blends using a design of experiments approach†

Scott Wiseman, Christian A. Michelbach, Hu Li and Alison S. Tomlin

Acid-catalysed alcoholysis of lignocellulosic biomass produces a tailorable advanced biofuel blend, with the primary products being an alkyl levulinate, a dialkyl ether, and alcohol. Varying process parameters during production has the potential to produce differing quantities of the three components, affecting both physical and combustion properties. Starting alcohols, ethanol, *n*-butanol, and *n*-pentanol were chosen to investigate the effects of carbon chain length on the physical properties of model ethyl, butyl, and pentyl-based blends, produced from alcoholysis. Blends were designed to contain ≥50 vol% alkyl levulinate, with the remainder composed of the corresponding ether and alcohol. Existing fuel standards set limits for different physical and chemical properties that should be met to enhance commercial viability. In the present work, the flash point, density at 15 °C and kinematic viscosity at 40 °C (KV40) were measured for a range of three-component blends. The study also investigated the impact of diesel (EN 590 compliant) blending on these properties, at 0–95% volume diesel. A design of experiments approach selected optimal blends for testing and was used to develop predictive physical properties models based on polynomial fits. The predictive models for the properties of the three-component blends had average absolute relative deviations <5%, indicating their utility for predicting generalised blend properties. The models facilitated the determination of blend boundaries, within which the formulations would meet existing fuel standards limits. Flash points ranged from 26–57 °C and 54–81 °C for the butyl and pentyl-based blends without diesel, respectively. Densities at 15 °C ranged between 0.879–0.989 g cm^{-3}, 0.874–0.957 g cm^{-3}, and 0.878–0.949 g cm^{-3} for the ethyl, butyl and pentyl-based blends without diesel, respectively. The KV40 ranged from 1.186–1.846 mm^2 s^{-1} and 1.578–2.180 mm^2 s^{-1} for butyl and pentyl-based blends without diesel, respectively. Butyl-based blends with diesel were found to be the most practically suitable and met the BS 2869 density limits.

Received 26th June 2023
Accepted 27th September 2023

DOI: 10.1039/d3se00822c

rsc.li/sustainable-energy

Introduction

In 2019, the transport sector was one of the largest contributors to global greenhouse gas emissions. It accounted for 29% of the total emissions in the United States, 23% of the total net emissions (including international transport) for the European Union, and 27% of the total emissions in the United Kingdom (UK).[1–5] Whilst new light-duty vehicles are likely to be electrified in the near future, the decarbonisation of the used vehicle market may take considerably longer, given the prevalence of road-worthy internal combustion engine vehicles. Significant challenges are also present in the development of alternative powertrains for heavy-duty vehicles, indicating that their reliance on liquid fuels (in most cases diesel) is also likely to continue. Therefore, in order to achieve decarbonisation targets in these sectors, low-carbon 'drop-in' fuels are required as alternatives to traditional fuels.[1–3] Biofuels are one potential solution, but the negative effects of land use change and food crop competition have rightfully limited their production and utilisation. European legislation, as part of the Revised Renewable Energy Directive (RED II), limits the use of biofuels produced from food and feed crops to 7% of total energy consumption within the transport sector for a member state by 2030.[6] RED II further promotes non-food crop advanced biofuels, stipulating that advanced biofuels produced using lignocellulosic Annex IX feedstocks should contribute at least a 3.5% share of the energy consumption in the transport sector by 2030.[6]

The conversion of lignocellulosic material into advanced biofuels needs to be cost-effective and sustainable to ensure their competitiveness with the fossil fuel they displace.[7] To be considered viable short-term alternatives, these fuels must be

School of Chemical and Process Engineering, University of Leeds, Leeds, LS2 9JT, UK

† Electronic supplementary information (ESI) available: Model coefficients and experimental data. See DOI: https://doi.org/10.1039/d3se00822c

compatible with existing vehicles and fuel storage and delivery infrastructure to be considered 'drop-in' fuels. Depending on the production process used, a range of potential biofuel blending components could be viable. However, assessing a range of fuel properties will be required to contribute to the assessment of their compatibility.

Alcoholysis of lignocellulosic biomass is a potentially attractive advanced biofuel production method, which can produce tailorable advanced biofuel blends. Each blend consists of three main products: an alkyl levulinate ester from the conversion of cellulose (where the alcohol used dictates the ester formed), a dialkyl ether from the alcohol undergoing acid-catalysed etherification, and the starting alcohol used.[8–10] The product blend may be tailored by utilising different reaction conditions to favour dialkyl ether or alkyl levulinate production.[8,9] The production of a tailorable blend provides the opportunity to produce fuel blends that could comply with existing fuel standards. This could further enhance their commercial and practical viability.

Fuels sold in the UK and Europe must meet a range of physical property limits specified by various fuel standards. Diesel must meet the requirements of EN 590, biodiesel (fatty acid methyl ester (FAME)) must likewise meet EN 14214 specifications, and BS 2869 gives limits for 'A2—automotive distillate fuel for non-road mobile machinery', such as red diesel.[11–13] Red diesel can only be used in specific applications, such as the off-road sectors of agriculture and construction, and off-grid power generation.[14] Not only are there differences in the physical properties between an EN 590 diesel and a BS 2869 red diesel due to the different limits, but there can also be chemical differences between the two. For example, there are limits for the polycyclic aromatic hydrocarbons (PAH) content in EN 590 of 8% by mass, whereas BS 2869 has no limits for PAH content.[12,13] This increased aromatic content can increase particulate matter emissions, but it may also increase the miscibility of polar blend components, such as oxygenated biofuels like ethyl levulinate as Christensen *et al.*[15] demonstrated with the improved miscibility of ethyl levulinate in diesel fuels with greater aromatic fractions.[15,16]

Production of advanced biofuel blends that meet the limits of these fuel standards would allow advanced biofuels to be developed and utilised without adapting current infrastructure. However, currently, the addition of any of these advanced biofuel components to a diesel base fuel will result in a fuel blend that is non-compliant since EN 590 and BS 2869 state that the only oxygenated biofuel species that can be added is FAME up to 7% volume.[12,13] If it can be demonstrated that property limits, other than biofuel content, can be met with advanced biofuel blends with and without diesel, this would support the need to adapt existing fuel standards to allow for the utilisation of oxygenated advanced biofuels.

The development of predictive models for a subset of standardised physical properties and understanding how they change with blend composition, was the focus of this study due to their implications for fuel handling, storage, and engine performance. There are many other physical properties that are influential on the performance of a fuel that can be readily calculated using linear blending laws, such as the lower heating value and oxygen content, with examples for selected blends shown in ESI S1.† However, these properties do not have standard limits for diesel applications.[12,13] There are also other properties that can be adjusted with additives to ensure the standard limits are met, for example the pour point or total acid number of the blend. This study however, focused on properties that affect fuel spray, handling and safety and may not be readily calculated using linear blending rules. Hence, the use of a design of experiments (DoE) methodology for developing predictive models for blend properties was tested. The chosen properties were the flash point, the density (at 15 °C), and the kinematic viscosity at 40 °C (KV40).[17–22] An understanding of the compositional effects on the flash points is needed for the safe storage and handling of fuels, as it is the lowest temperature at which a flammable vapour is formed.[20,21] Density and KV40 were primarily of interest due to their impact on spray dynamics and atomisation during fuel injection and the resultant influences on ignition delay times and emissions.[17,23] The higher the densities and viscosities, the larger the fuel droplets; potentially resulting in rich regions in the cylinder that generate more soot.[17] Density limits are an additional measure to control the PAH content, as PAHs are denser than alkanes. Controlling PAH content contributes to reducing particulate matter emissions from engines. However, using oxygenated biofuels would reduce the total PAH content and therefore potentially reduce particulate emissions relative to diesel.[24] Tight density limits could prevent the use of some potential advanced biofuel components who's addition would not necessarily have a negative influence on particulate emissions. The KV40 limit is in place to ensure adequate fuel pump lubrication during engine operation.[17–19] The limits for these properties from the three standards are summarised in Table 1.

Due to the nature of the alcoholysis process, the products (and therefore the blend properties) depend on the starting solvent and the product composition. To determine the effects of carbon chain length on the fuel's physical properties, model biofuel blends derived from three alcohol solvents of increasing chain length were investigated in this work: ethanol, *n*-butanol, and *n*-pentanol. The resultant three-component blends of ethanol (EtOH), ethyl levulinate (EL), and diethyl ether (DEE) will be termed the ethyl-based (Et) blends. Likewise, the butyl-based (Bu) blends refer to *n*-butanol (*n*BuOH), *n*-butyl levulinate (*n*BL), and di-*n*-butyl ether (DNBE) blends, while the pentyl-based (Pe) blends refer to *n*-pentanol (*n*PeOH), *n*-pentyl levulinate (*n*PL), and di-*n*-pentyl ether (DNPE). Fig. 1 shows the skeletal structures for each of these compounds.

Table 1 Physical properties limits from EN 590, EN 14214, and BS 2869[11–13]

Property	EN 590	EN 14214	BS 2869
Flash point (°C)	>55	>101	>55
Density at 15 °C (g cm^{-3})	0.820–0.845	0.860–0.900	>0.820
Kinematic viscosity at 40 °C (KV40) (mm^2 s^{-1})	2.0–4.5	3.5–5.0	2.0–5.0

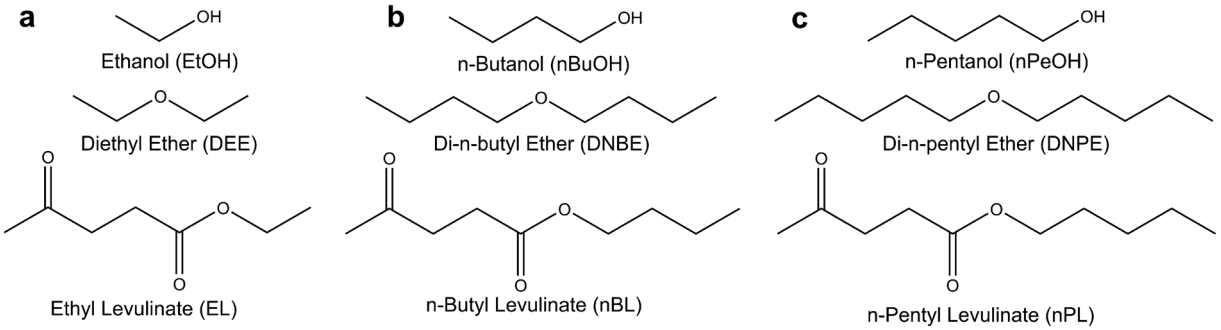

Fig. 1 Biofuel components. (a) Ethyl-based blends (Et). (b) Butyl-based blends (Bu). (c) Pentyl-based blends (Pe).

Diesel has a typical carbon chain length range of 10 to 24.[25–30] The use of longer carbon chain alcohols will result in alcoholysis products that have carbon chain lengths closer to those of typical diesel components, which is likely to favour the blending of the resulting advanced biofuel blend with diesel.

Studies have shown that using longer carbon chain length alcohols typically reduces the yield of the alkyl levulinate from the alcoholysis of lignocellulosic biomass.[31–34] Therefore, the production of *n*PL would require increased use of pentanol compared to ethanol for EL production, increased biomass feedstock requirements, and increased energy usage to produce large volumes.[31–34] However, an increased yield of alkyl levulinate indicates a more efficient conversion of biomass and a greater fraction of the energy extracted from the feedstock.[33] Furthermore, large-scale production of second-generation *n*-pentanol from lignocellulosic biomass is not yet viable, resulting in the production of an advanced pentyl-based biofuel blend still requiring fossil fuel derived feedstocks.[35,36] In contrast, *n*-butanol and ethanol can be produced through fermentation methods, including the acetone-butanol-ethanol fermentation method.[37,38]

The density of alkyl levulinates decreases as the carbon chain length increases, as reported by Schuette and Cowley,[39] whereas the density of alcohols and ethers increases as the carbon chain lengthens. Therefore, these effects should counteract each other when the components are blended and may enable there to be substantial fractions of the alkyl levulinate and dialkyl ether within blends that meet fuel standard limits. The effects of these interactions should be identified when generating the predictive models, as the coefficients will indicate the contribution of each component to the density. The flash points and KV40 of all the components increase as the carbon chain length increases.[15] A summary of the properties of the fuel blend components used in this work is provided in Table 2. Thermogravimetric analysis of the diesel used is presented in ESI (S1.2).†

Howard *et al.*[8] determined the derived cetane number (DCN) for a wide range of ethyl-based blends using an ignition quality tester following the ASTM D6890 test method and produced a predictive DCN blending model. The model was dependent on the DCN and mole fractions of each component, as well as three coefficients (per component) determined through linear regression.[8] The use of linear regression demonstrated that this methodology would be suitable to produce models for other physical and chemical properties. Their work determined the blend compositions that matched the DCN of typical diesel

Table 2 Summary of the properties of the fuel components used in this work

Fuel component	Purity	Supplier	Flash point[a] (°C)	Density at 15[b] °C (g cm^{-3})	Kinematic viscosity at 40[b] °C (mm^2 s^{-1})	Boiling point[c] (°C)
Ultra-low sulphur diesel (ULSD)		Crown oils	67	0.838	2.813	
Ethanol (EtOH)	>99%	VWR	16[d]	0.795	1.099	78
n-Butanol (*n*BuOH)	≥99.9%	Sigma Aldrich	35	0.811	2.261	118
n-Pentanol (*n*PeOH)	>99%	Sigma Aldrich	49	0.819	2.899	136
Diethyl ether (DEE) containing 1 ppm butylated hydroxytoluene	≥99.7%	Sigma Aldrich	−40[e]	0.720	—	35
Di-*n*-butyl ether (DNBE)	99+%	Fisher	25	0.768	0.736	142
Di-*n*-pentyl ether (DNPE)	>98%	VWR	57	0.789	1.131	183
Ethyl levulinate (EL)	99%	Sigma Aldrich	94	1.017	1.553	206
n-Butyl levulinate (*n*BL)	98%	Alfa Aesar	111	0.973	2.017	238
n-Pentyl levulinate (*n*PL)	>95%	AkoS	96	0.963	2.375	253[f]

[a] Measured using Setaflash Series 3 plus. [b] Measured using the Anton Paar SVM3000. [c] Obtained from ref. 40–48. [d] Obtained from ref. 40. [e] Obtained from ref. 43. [f] Obtained from ref. 39.

fuels, but they did not consider the physical properties of the blends. Since the alcoholysis products depend on the alcohol used, changing ethanol to a longer chain alcohol such as *n*-butanol or *n*-pentanol may produce biofuel blends that are more compatible with diesel, as properties of the individual biofuel components are closer to the diesel standards limits.

Limited studies have been conducted using *n*BL, DNBE, and *n*BuOH as a three-component biofuel blend. Antonetti *et al.*[10] studied the alcoholysis of *eucalyptus nitens* to the utilisation of a three-component model product blend (using the pure biofuel components) in a 2-cylinder, 21 kW diesel engine without physical properties testing. The blend composition used was 70 wt% *n*BuOH/20 wt% DNBE/10 wt% *n*BL and was blended into diesel at 10, 20, and 30 vol%.[10] The fractions of *n*-butanol and DNBE used by Antonetti *et al.*[10] are unlikely to produce blends that comply with EN 590 or BS 2869 due to the impact of *n*-butanol on flash points, as reported by Kuszewski,[49] and the properties of all three components illustrated in Table 2.[10,12,49] Flash points of multi-component blends typically tend towards that of the component with the lowest flash point, so the flash points of any significant blending components must be similar to that of diesel.[50,51] To reduce the need to test every possible blend composition and to be able to predict rapidly the physical properties of any blend composition, accurate, accessible, and appropriate physical properties models need to be available.

The density of multi-component mixtures can be predicted accurately using linear-by-volume blending rules, but the same is not true for flash points and viscosities.[52–56] Many models are available in the literature for predicting flash points.[53,54] However, many of these were designed using vapour–liquid equilibrium models such as the Liaw model or the Catoire model.[20,21,57] The Liaw and Catoire models require the use of activity coefficients for each species in the blend, and the most accurate models to determine the activity coefficients for mixtures are not readily and freely available.[20,21,57] The activity coefficients are dependent upon the nature of, and the amount of, different intermolecular interactions. As a result, they have to be calculated for each specific blend composition using models such as Universal Quasichemical Functional-group Activity Coefficients (UNIFAC) and modified UNIFAC.[57–61] The additional requirements to model the flash point of ternary advanced biofuel blends make the development and use of simple polynomial equations more attractive. Liaw *et al.*[62] demonstrated that the flash points of ternary mixtures depend upon the molecular interactions between the blend components, with more favourable interactions increasing the flash points.[57–61]

The viscosity of multi-component blends also typically displays a non-linear relationship with the change in the fractions of constituents. Several models are available for predicting the viscosity of binary blends, including the Grunberg–Nissan equation, Bingham, and Latour equations.[52] The Grunberg–Nissan equation requires an interaction parameter to account for intermolecular interactions and non-ideal mixture behaviour, such as those that arise for mixtures of alcohols with diesel, and is entirely mixture dependent.[17,63] Lapuerta *et al.*[17] demonstrated that the Grunberg–Nissan equation can accurately predict viscosities for diesel and *n*-butanol mixtures as their model fitted experimental data with an R^2 value of 0.9894. They used an interaction coefficient determined in their previous work, where they also produced an empirical relationship for calculating the interaction coefficient of alcohol and diesel blends based on the number of carbon atoms in the alcohol.[19] Mixtures with three or more components have interactions that are more complex. The interaction parameters for such mixtures also are not readily available in the literature and can be difficult to obtain experimentally, making predicting the viscosity accurately potentially difficult for novel fuel blends. The viscosity models of the three-component mixtures studied in this work were simple polynomial models and did not require these interaction terms as they are fitted to response surfaces.

Due to the complex nature of the intermolecular interactions in ternary mixtures, there are no simplistic and easily accessible physical properties models available, especially for flash point and viscosity, where the effects of the intermolecular interactions need to be accounted for. The development and utilisation of accurate models would allow for the prediction of properties for untested blends, enabling the rapid screening of different blend compositions more efficiently without extensive experimental measurements. This study, therefore, aims to produce accurate polynomial models to predict the physical properties of the different ternary advanced biofuel blends, to characterise the effect of blend composition on densities at 15 °C, flash points, and KV40, and to investigate the impact of carbon chain length on these properties using a DoE approach. The development of polynomial models is more efficient, cost-effective, and sustainable through utilising a DoE approach as it determines the optimal blends to test for a given number of experiments, thus reducing testing time, volumes of cleaning solvents and biofuel components used. These models can then be used to aid fuel formulation to produce blends that meet the limits set in fuel standards. If accurate models can be produced for the selected physical properties using the DoE approach, it could be applied to produce models for other properties that fuel blends are required to meet in comparison to relevant standards.

Methodology

Fuel blending

The studied biofuel mixtures were blended volumetrically and were designed to contain at least 50% alkyl levulinate, with the remaining volume fraction consisting of the associated alcohol and dialkyl ether. The blends will be denoted by the prefixes Et, Bu, and Pe to distinguish the alcohol precursor for the ethyl, butyl, and pentyl-based blends, respectively, followed by the ratio of the alkyl levulinate : dialkyl ether : alcohol volume fractions in vol%. For example, Bu-70 : 25 : 5 is a blend of 70 vol% *n*BL, 25 vol% DNBE, and 5 vol% *n*BuOH, and D50Bu50 – 70 : 25 : 5 is the same three-component blend blended with 50 vol% ULSD. Utilising high alkyl levulinate fractions could make the alcoholysis process more economically viable, as it indicates a greater conversion of the biomass, and upgrading of the alcohol, producing more of the target product.[64]

When producing the sample blends, components were blended in order of volatility (from least to most volatile), stoppering the sample vial between each addition, and mixed manually by shaking the vessel for one minute. The tolerance for the production of the blends was ±5% of the required volume of each component. To minimise the errors when producing the blends, the sample vials were weighed after the addition of each component. The components used and their properties are listed in Table 2. All blends were prepared the previous day to ensure that mixtures were stable and completely miscible, with immiscible blends discarded. The *n*-pentyl levulinate used in this study contained 1.8 vol% *n*-pentanol as an impurity. Although it was a small fraction, the presence of *n*-pentanol was expected to reduce the flash point of the *n*PL used and the blends due to its lower flash point and its presence decreasing the mean carbon chain length, following the trend observed for the other biofuel components in Table 2. This fraction of *n*-pentanol was accounted for during mixture blending to ensure the compositions consisted of the correct volume fractions.

Design of experiments approach

Model construction. For the production of the physical properties models, a DoE approach was utilised using Sartorius Stedim's MODDE (Modelling and Design).[65] This approach and software were applied to determine the optimal biofuel blend compositions within the experimental design space for testing, to produce predictive polynomial models, and to determine blend boundaries where the composition space of the biofuel blends meets the property limits specified in the fuel standards. The first step was to conduct an initial screening to cover a large area of the design space. This consisted of 10 blends and 12 runs, with two runs being duplicates. After the screening, there was model optimisation to ensure the models generated were accurate.

The polynomial models fitted by MODDE are shown in eqn (1) and (2), for the linear and quadratic forms, respectively.

$$y = C + b_1x_1 + b_2x_2 + b_3x_3, \quad (1)$$

$$y = C + b_1x_1 + b_2x_2 + b_3x_3 + b_{12}x_1x_2 + b_{13}x_1x_3 + b_{23}x_2x_3 + b_{11}{x_1}^2 + b_{22}{x_2}^2 + b_{33}{x_3}^3, \quad (2)$$

where y is the property of interest, C is a constant, b_{ii}k are the coefficients, including those accounting for interactions between components, and x_1, x_2, and x_3 are the volume fractions of the alkyl levulinate, dialkyl ether, and alcohol, respectively. The model coefficients were defined using a hierarchical approach with the constant term being at the top of the hierarchy, followed by the linear terms, and finally the quadratic terms. This results in the coefficients being defined as relative to the designated reference mixture, as opposed to a standard approach wherein coefficients are defined based on the values of pure components. The reference mixture was the centre point of the blending space, as shown in Fig. 2.

Model optimisation. The DoE was optimised using a complemented design and the D-optimal algorithm to improve the model fit, confirm component interactions, or resolve non-linearities.[65,66] This takes the screening design space and determines additional experiments which aid the model fit, enabling the quadratic and cubic models to be fitted with lower fitting errors.[65] The D-optimal algorithm maximises the value of the determinant of the model information matrix, which is inversely proportional to the variance-covariance matrix.[65–70] Hence, maximising the determinant of the information matrix should reduce the variance in the calculations of the coefficients, as the greater the number of experiments, the easier it is to obtain the largest determinant.[65–70] The D-optimal algorithm in MODDE finds the maximum determinant possible for the number of runs stated.[65,68]

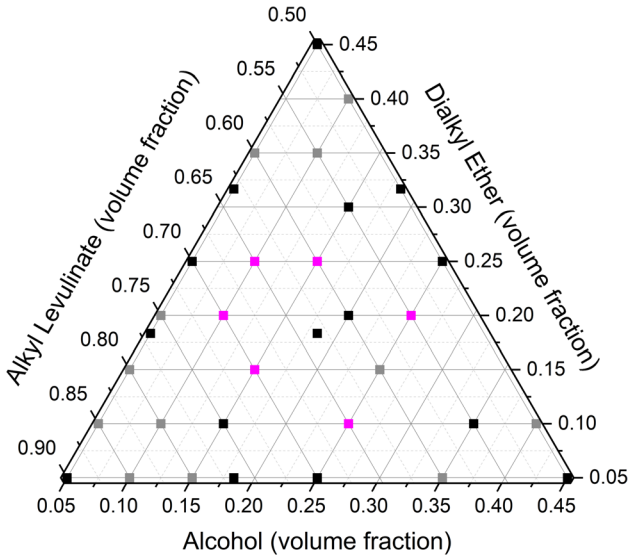

Fig. 2 Blends tested in the design space. Black squares show MODDE generated blends, grey squares represent additional blends added to increase coverage, and magenta squares show blends used for final model evaluation.

The quality of the model fits was assessed using the R^2 value, *p*-values of each coefficient, *p*-values of the model and lack of fit of the model, and the average absolute relative deviation (AARD %) between the measured value and the predicted value, calculated using eqn (3).

$$\text{AARD } \% = \frac{1}{n}\sum_{i=1}^{n}\frac{|y_{\text{exp}} - y_{\text{pred}}|}{y_{\text{exp}}} \times 100\% \quad (3)$$

where y_{exp} was the experimentally measured value, y_{pred} is the predicted value, and n is the number of experiments conducted. This was used to ensure that any over-predictions did not negate any under-predictions.

Ternary biofuel blends tested. The blend compositions tested to produce the predictive models are shown in Fig. 2. In this figure, the black squares represent the original blends tested to produce a preliminary model: 10 screening blends and 5 optimisation blends with 6 replicates. The grey squares show the second round of experiments conducted as validation of the initial models, which were then incorporated into the model fitting due to poor predictability in some regions of the design

space. The magenta squares show blend compositions that were used as final model validation to test the regions of the design space where blends were not tested.

Miscibility testing. To assess the long-term miscibility of the fuel blends, 20 cm^3 of the blends, with and without diesel, were stored for 3 months in graduated test tubes at ambient temperatures (18–21 °C) and refrigerated at 3 °C. Visual inspections of the test tubes were conducted to detect any separation and noticeable changes, such as deposit formation, with the immiscible blends removed from further physical properties testing. Any deposits that form could result in fuel filter and fuel line blockages, as well as potentially changing the injected fuel blend composition, resulting in changes to the engine performance and emissions.

Flash point. Flash points were measured using a Stanhope Seta Setaflash Series 3 Plus, following EN ISO 3679.[71] The Setaflash Series 3 Plus is a small-scale closed cup flash point tester. Samples of 2 cm^3 were injected into the sample cup and heated at a rate of 2 °C min^{-1}. A test flame was then dipped into the vapour space every 1 °C until a flash is detected by the flash detector. EN ISO 3679 has a repeatability limit of $0.0152(X + 110)$ °C, where X is the measured flash point.[71] The main source of error in the test was due to mixture preparation but the 5% tolerance for the fuel blending and the weighing of blends throughout their production reduced this error. Mixtures were prepared the day before testing, to ensure mixture stability and homogeneity, as determined by visual inspection, to ensure repeatability of the measurements.

Kinematic viscosity at 40 °C. The KV40 was measured using an Anton Paar SVM3000 Stabinger Viscometer, following BS EN 16896.[72] A 5 cm^3 sample was injected through the viscometer for every three measurements of the KV40. The viscometer measured dynamic viscosity and density at the set temperature, which were used to calculate kinematic viscosity as the ratio of dynamic viscosity to density. The SVM3000 has a repeatability of 0.09% for the KV40 measurements, and BS EN 16896 has a repeatability limit of $0.0105–0.0003X$ mm^2 s^{-1}, where X is the measured KV40.[72] One of the sources of error was likely the mixture preparation, although these were minimised using the steps for fuel blending discussed previously. An additional possible source of error could arise during the injection of the sample into the viscometer, as there needed to be no air bubbles in the syringe. To minimise this error, the syringe was inverted and left to allow all the air bubbles to rise to the surface before evacuating the air from the syringe and ensuring the tip was filled with the sample.

Density at 15 °C. The density at 15 °C of the ethyl and butyl-based three-component blends was measured following ISO 3838: a pycnometer method, using 5 cm^3 capillary stopper pycnometers.[73] The density at 15 °C of the blends of diesel with the butyl-based three-component blends and the pentyl-based three-component blends were measured using an Anton Paar SVM3000 Stabinger Viscometer following ISO 12185.[74] As with the measurement of KV40, 5 cm^3 of the sample was injected through the viscometer for every three measurements of the mixture density. The difference between measured densities of the same blends using both methods was <1%. The ISO 12185 methodology was used as it required less sample and was more time effective. The SVM3000 has a repeatability limit for density measurements of 0.0001 g cm^{-3}, which is lower than the ISO 12185 repeatability limit of 0.0002 g cm^{-3}, and the ISO 3838 method has a repeatability limit of 0.0007 g cm^{-3}.[73,74]

Results and discussion

Three-component blend properties

All ethyl, butyl, and pentyl-based three-component biofuel mixtures were completely stable before and during the measurement of the physical properties, and hence all required tests could be completed. In contrast, blends with ULSD exhibited different stability behaviours depending on the carbon chain length of the biofuel components, and this is discussed further in the Blends with diesel section. The model parameters are presented in S2–S4 of the ESI.† All of the experimental results and model predictions shown in the parity plots, are presented in tabular form in ESI S5.† In S5,† experimental errors are the standard deviations of three repeated measurements, and errors reported for predicted values are the model's 95% confidence intervals.

Density at 15 °C of the three-component blends

Densities at 15 °C ranged between 0.879–0.989 g cm^{-3}, 0.874–0.957 g cm^{-3}, and 0.878–0.949 g cm^{-3} for the ethyl, butyl, and pentyl-based blends, respectively, as shown in Fig. 3. The density of all the three-component blends was above the EN 590 maximum of 0.845 g cm^{-3}, regardless of the blend composition.[12] This is due to the high densities of the alkyl levulinates, which were used with a 50% minimum volume fraction in this study, and the expected linear blending laws for density. On the other hand, the density limits of BS 2869 can be achieved for all blends, as there is only a minimum limit of 0.820 g cm^{-3}.[13] Blends containing up to 57 vol% of EL, 60 vol% of *n*BL, and 62 vol% *n*PL are also within the EN 14214 density limits.[11] Being able to meet the limits in the other fuel standards indicates that such biofuel blends may be viable as fuels for agricultural, domestic, or industrial engines, but more information is required on their physical and combustion properties before such a conclusion can be stated definitively. Fig. 3 shows that despite the change in the carbon chain length for the different starting alcohols, the densities remain relatively similar when the alkyl levulinate fraction is <65 vol%. However, the densities of the blends with >80 vol% alkyl levulinate decrease as the carbon chain length increases due to the reducing densities of the alkyl levulinate (the largest fraction of the blend) as the carbon chain length increases. This occurs even with the increasing densities of the alcohol/ether as the carbon chain length increases (Table 2).

Exceeding the upper density limits specified by fuel standards can affect the fuel injection spray dynamics. Kim *et al.*[23] showed that fuels with a higher density have a greater spray penetration, which requires an increased mixing time to allow for fuel vaporisation, increasing the ignition delay times. The resultant presence of fuel rich zones may increase incomplete

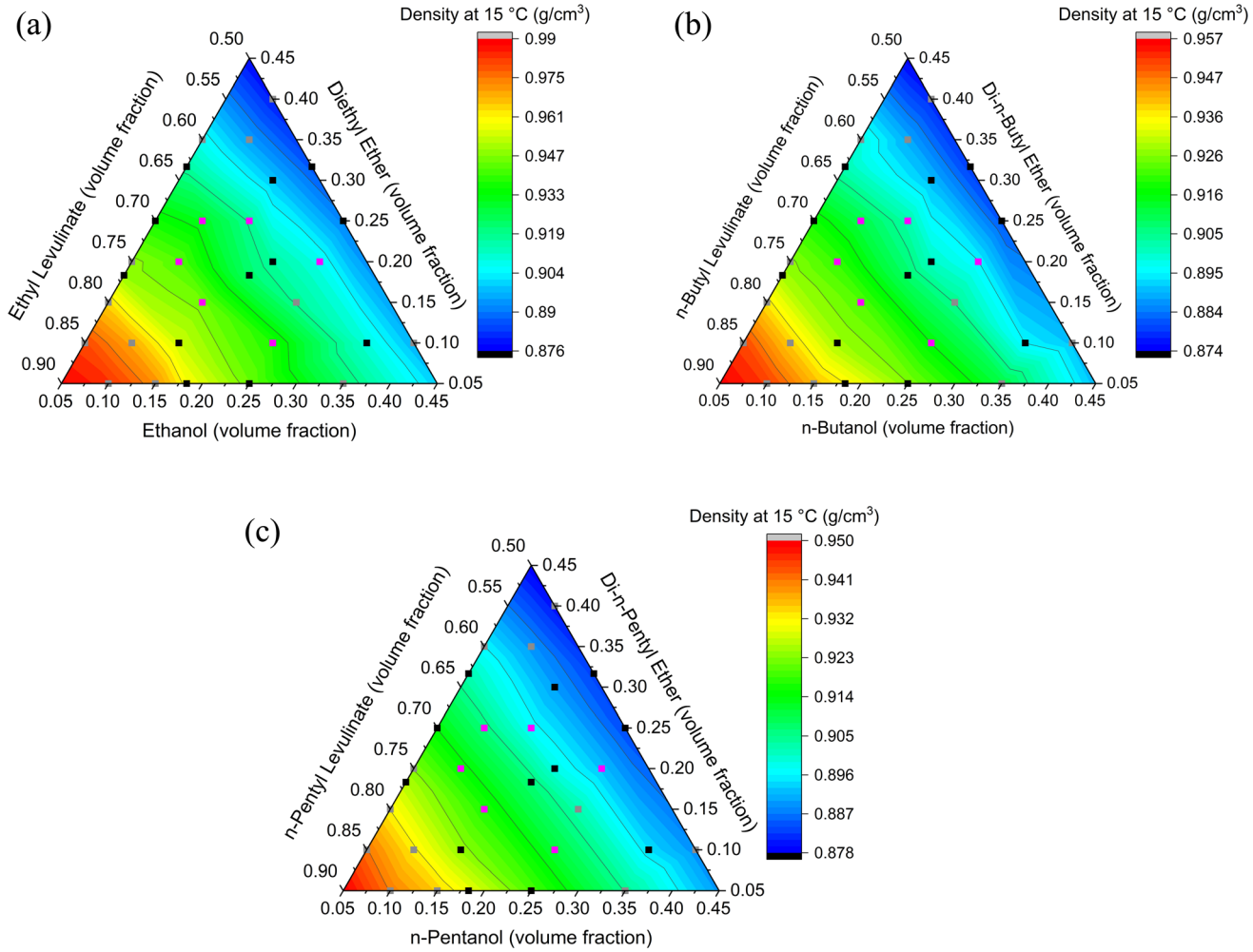

Fig. 3 Density at 15 °C: experimental ternary diagrams for the three-component biofuel blends. (a) Ethyl-based blends. (b) Butyl-based blends. (c) Pentyl-based blends. Black squares: MODDE generated blends, grey squares: additional blends added to increase coverage, and magenta squares: blends used to test the models.

combustion, resulting in elevated soot, hydrocarbon (HC), and CO emissions. Poor mixing would also create lean zones in the cylinder, which could increase nitrogen oxide ($NO_X = NO + NO_2$) emissions.[75] However, the most significant implication of a higher density is the resultant change in the mass of fuel injected if the operational parameters of an engine are not modified to compensate. Fuel injection is commonly performed on a volumetric basis, hence the use of fuel with a higher density will result in a greater mass of fuel injected.[53] If the molar mass of the biofuel blend is similar to that of standard diesel, a significant increase in density will also produce a change in fuel/air stoichiometry towards richer combustion. Therefore, to ensure the same engine performance and limit the emissions of incomplete combustion products, the injection parameters (such as volume) may need to be modified. Determining optimal engine and fuel injection parameters would require a separate study, as modifications based solely on physical properties (such as density) may cause adverse combustion effects. For example, a reduction in injected volume to compensate for a higher density will also lower the energy available per cycle; a problem that will be exacerbated by the lower energy density of oxygenated biofuel components.[53]

A linear density model provided the most accurate predictions for all blending regimes investigated. R^2 values of 0.996, 0.977, and 0.998 were obtained for the ethyl, butyl, and pentyl-based blends, respectively. The AARD% for the ethyl, butyl, and pentyl-based blends are 0.25%, 0.22%, and 0.05%, respectively, indicating good agreement between the predicted and experimental values. This is also shown by the concentration of data around the $y = x$ line in the parity plots shown in Fig. 4. All terms in the density models are significant, with p-values <0.05. A full summary of the coefficients and their p-values can be found in ESI S2.1–S2.3.†

Comparing the linear-by-volume blending law for density and the fitted MODDE linear models for the ethyl, butyl, and pentyl-based blends displays a good agreement, with AARD% being 0.47%, 0.32%, and 0.07%, respectively. Fig. 5 shows a comparison between the predictions of the MODDE-generated model and the linear blending rule. The ethyl-based blends show a deviation at lower densities, which is representative of

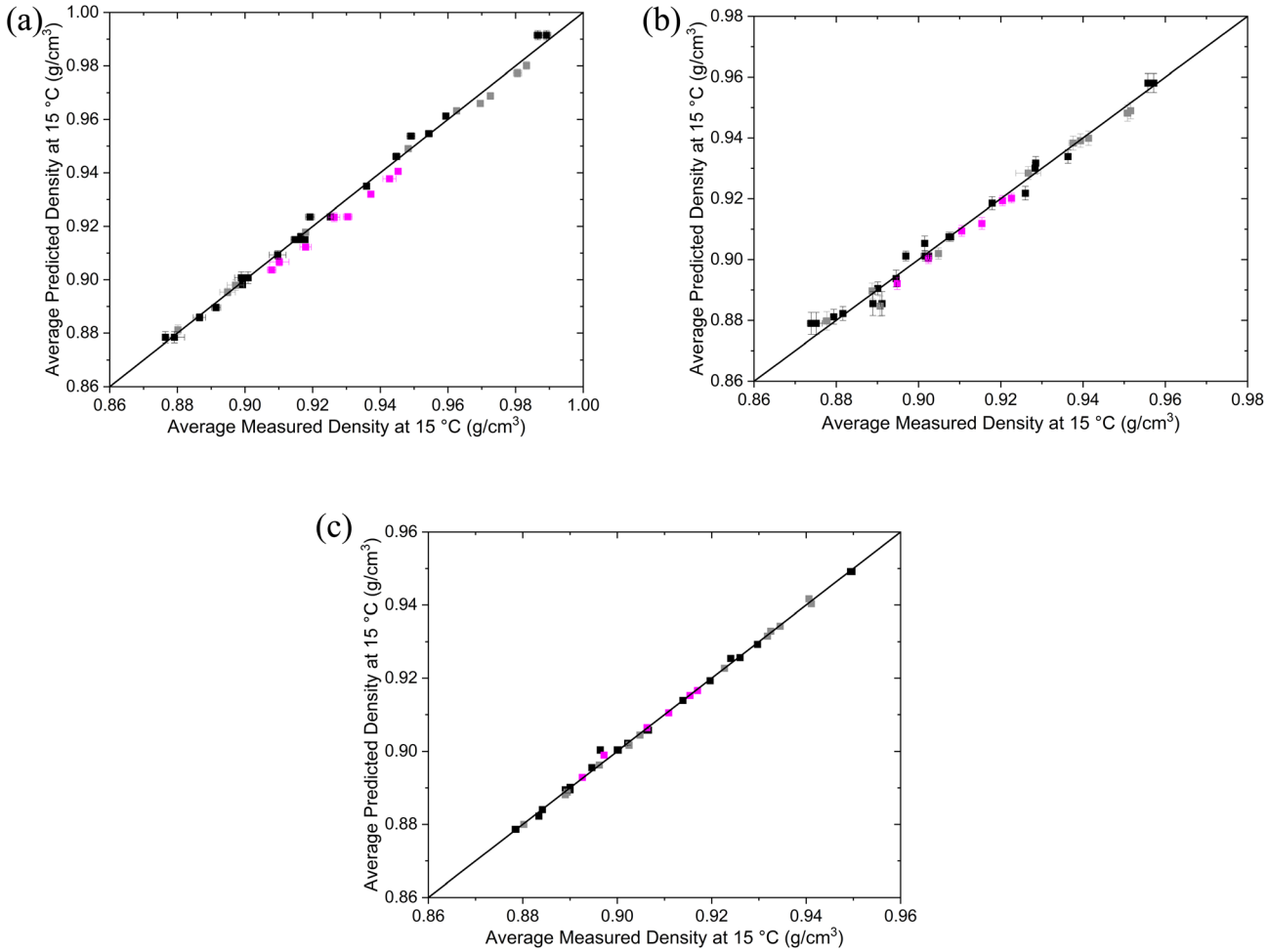

Fig. 4 Parity plots of the density at 15 °C with linear model predictions from MODDE for (a) ethyl-based blends, (b) butyl-based blends, (c) pentyl-based blends. Black squares: MODDE generated blends, grey squares: additional blends added to increase coverage, and magenta squares: blends used to test the models.

an increase in experimental error due to the high volatility of DEE. This error increased for larger DEE fractions, as the potential for evaporative losses during sample handling produced higher compositional uncertainties. Overall, however, the results support using both the linear-by-volume blending rule and DoE models for predicting densities for mixtures of this type. The benefit of the DoE model is that it can be used in MODDE simultaneously with the other properties models to determine the blend boundaries for compliant blends.

Flash points of the three-component blends

The flash points of EtOH and DEE are below room temperature at atmospheric pressure (Table 2), making it impossible to collect flash point data for these using the Setaflash Series 3 plus. When DEE and EtOH were each blended at small fractions (<5% by volume) into ULSD, flash points were detected at room temperature. However, due to higher blending volumes, it is likely that blends with EtOH and DEE investigated in this study were likely to have flash points below room temperature and thus outside of the measurable regime. The flash point of the Et-90 : 5 : 5 blend was also at room temperature. Therefore, it was unlikely that blends with increased fractions of DEE or EtOH would produce measurable flash points.

Catoire *et al.*[51] demonstrated that the flash point of a blend is typically around the lowest individual flash point out of the blend components. Therefore, it would be expected that the flash points for the butyl-based blends would be approximately 25 °C (the flash point of DNBE) when there is a significant fraction of DNBE. For pentyl-based blends, the flash points should be close to 49 °C due to the influence of *n*-pentanol. The flash points of the butyl-based three-component blends ranged from 26–57 °C, with the flash point above 55 °C being attributed to the Bu-90 : 5 : 5 blend, as shown in Fig. 6a. The butyl-based blends would likely need to be blended with a high flash point diesel to achieve the minimum flash point required for EN 590 and BS 2869. However, the fractions at which they would still be compliant need to be determined.[12,13] This is discussed in the Blends with diesel section.

Flash points of the pentyl-based blends ranged from 54–81 °C, as shown in Fig. 6b. To produce flash points above 55 °C, the pentyl-based blends must contain ≥60 vol% *n*PL, with the

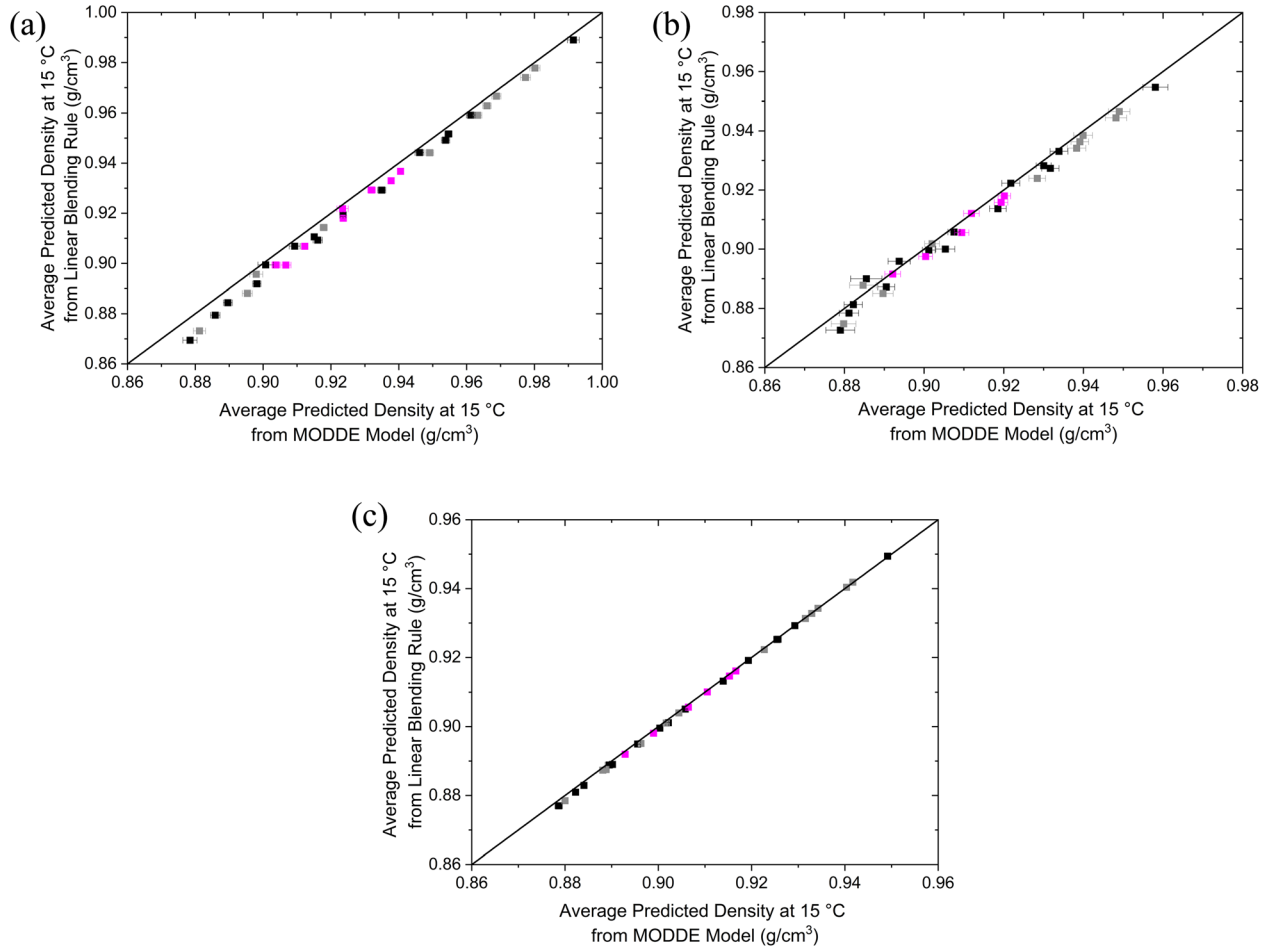

Fig. 5 Plots of the density at 15 °C based on linear models generated by MODDE *vs.* the density from the linear blending rule for (a) ethyl-based blends, (b) butyl-based blends, (c) pentyl-based blends. Black squares: MODDE generated blends, grey squares: additional blends added to increase coverage, and magenta squares: blends used to test the models.

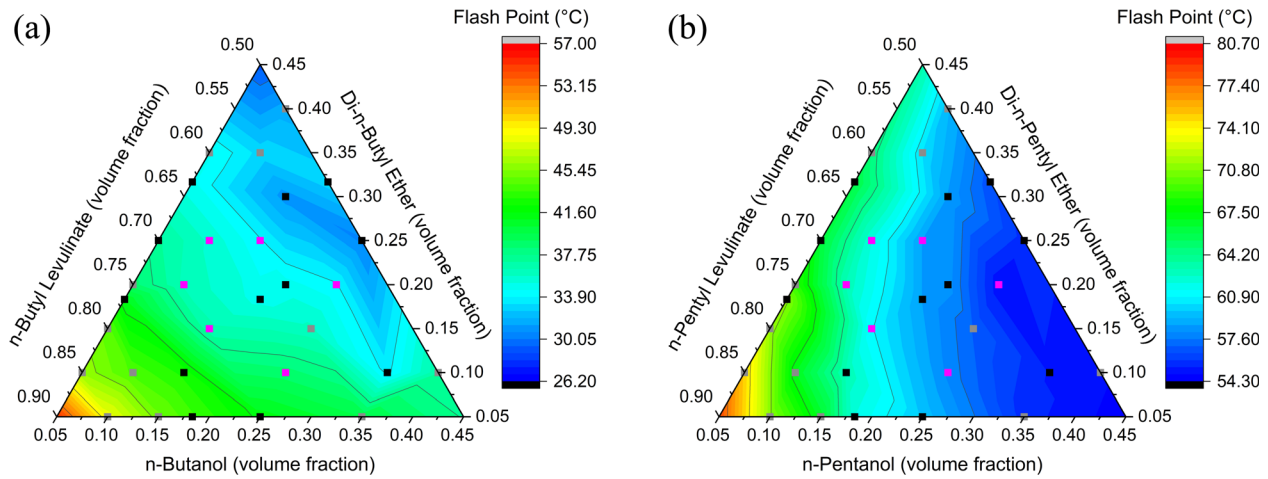

Fig. 6 Flash point experimental ternary diagrams for the three-component biofuel blends. (a) Butyl-based blends, (b) pentyl-based blends. Black squares: MODDE generated blends, grey squares: additional blends added to increase coverage, and magenta squares: blends used to test the models.

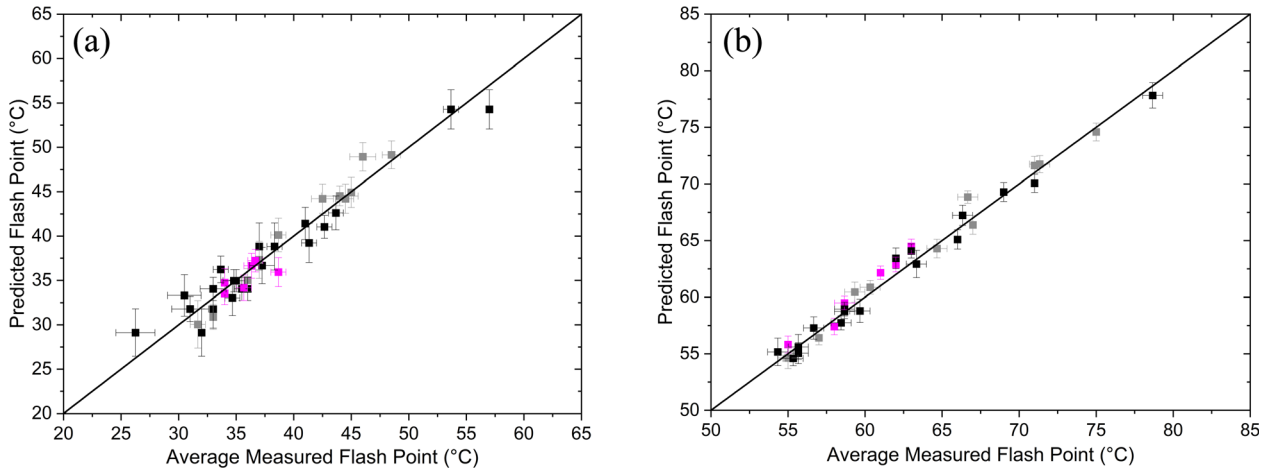

Fig. 7 Parity plots of the flash point quadratic models generated by MODDE for (a) butyl-based blends, (b) pentyl-based blends. Black squares: MODDE generated blends, grey squares: additional blends added to increase coverage, and magenta squares: blends used to test the models.

remaining fraction composed of any combination of DNPE and *n*PeOH. The pentyl-blend flash point was extensively affected by the fraction of the *n*PeOH present, as demonstrated in Fig. 6b, where the lower flash points are in the regions of higher *n*PeOH fractions. Unlike *n*BuOH in the butyl blends, *n*PeOH has the lowest flash point of the three components, and thus this reduction with the higher *n*PeOH fractions follows the observation of Catoire *et al.*[51]

The flash point of the blends increases as the carbon chain length increases. Increasing the carbon chain length causes an increase in boiling point for the investigated species, which results in a decrease in volatility and a higher temperature required to produce a flammable vapour. The resultant increase in flash points produces pentyl-based blends that are capable of meeting the EN 590 and BS 2869 fuel standard requirements for the flash point.[12,13] This implies that pentyl-based blend handling and storage may be compliant with existing infrastructure for this property. In regards to the required safety standards for such liquids, blends with flash points above 60 °C can be handled as a combustible liquid, in a similar manner to diesel, and those below 60 °C must be handled as a flammable liquid.[76]

Quadratic polynomial models were the most suitable for predicting flash points of the butyl and pentyl-based blends, with R^2 values of 0.924 and 0.982, respectively, indicating good agreement between predictions and experimental values (Fig. 7). The choice of the quadratic model is further validated when comparing the statistical parameters for all the fitted models, which are presented in ESI S3.1.† The AARD% between experimental and calculated values are 3.50% and 1.18% for the butyl and pentyl-based blends, respectively.

In the quadratic model for the butyl-based blends, the linear term in *n*BuOH was statistically insignificant, with a *p*-value of 0.11. However, it is clear from Fig. 6a that there is an influence of *n*BuOH on measured flash points but that the extent of its influence depends on the fractions of the other components. For example, for low fractions of DNBE and high fractions of *n*BL, the flashpoint decreases rapidly as *n*BuOH increases up to 10% but thereafter flattens off as *n*BuOH increases further. At higher fractions of DNBE, its effect on the flash point is stronger compared to the other components. This is likely due to *n*BL and DNBE having the extremes of the flash points, so they dominate the blend's flash point, and the influence of *n*BuOH is suppressed. Hence, the *n*BuOH linear term was kept in the model, as it could not be removed due to the model hierarchy. Interaction terms involving *n*BuOH and DNBE/*n*BL are shown to be significant in Table S3.1.2† which reflects these nonlinear responses. All the model terms in the flash point model for the pentyl-based blends were statistically significant, with *p*-values <0.05. A full summary of the *p*-values of the model terms is given in ESI S3.2.†

Kinematic viscosity at 40 °C of the three-component blends

Due to the relatively low boiling point of DEE (35 °C), the KV40 of the ethyl-based three-component blends cannot be measured as DEE would boil and evaporate, resulting in the loss of DEE and a binary biofuel blend of ethanol and EL being formed. This further indicates that the ethyl-based blends are unlikely to be suitable drop-in diesel alternatives, given the requirements of diesel fuel standards.[11,12]

The KV40s for the butyl-based blends range from 1.186–1.846 $mm^2\ s^{-1}$ (Fig. 8a), while the KV40s for pentyl-based blends range from 1.578–2.180 $mm^2\ s^{-1}$ (Fig. 8b). All of the butyl-based blends investigated in this study are below the 2.00 $mm^2\ s^{-1}$ minimum in EN 590 and BS 2869 and the EN 14214 minimum of 3.5 $mm^2\ s^{-1}$, regardless of the blend composition, as shown in Fig. 8a.[11–13] Therefore, the fraction of biofuel that can be blended with diesel and still comply with the fuel standards will depend on the viscosity of the diesel used.[12,13] Viscosities below the standard requirements will have implications for fuel delivery systems, particularly the lubrication of fuel pumps, potentially leading to increased wear and friction of the fuel delivery system.[17–19] Kim *et al.*[23] found that decreased fuel viscosity decreases the droplet Sauter mean diameter by

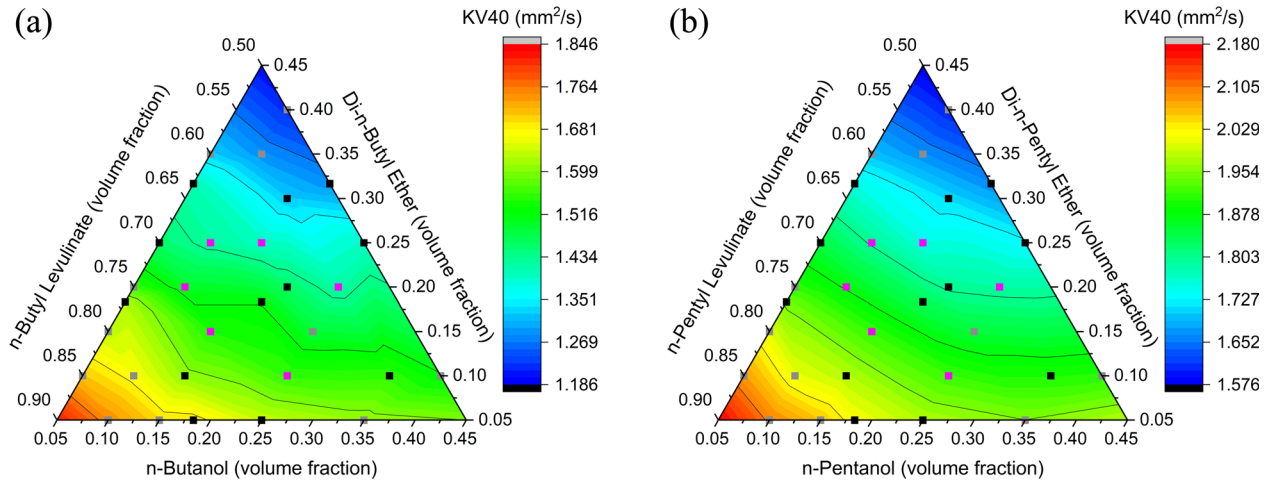

Fig. 8 Kinematic viscosity at 40 °C: experimental ternary diagrams for the three-component biofuel blends. (a) Butyl-based blends, (b) pentyl-based blends. Black squares: MODDE generated blends, grey squares: additional blends added to increase coverage, and magenta squares: blends used to test the models.

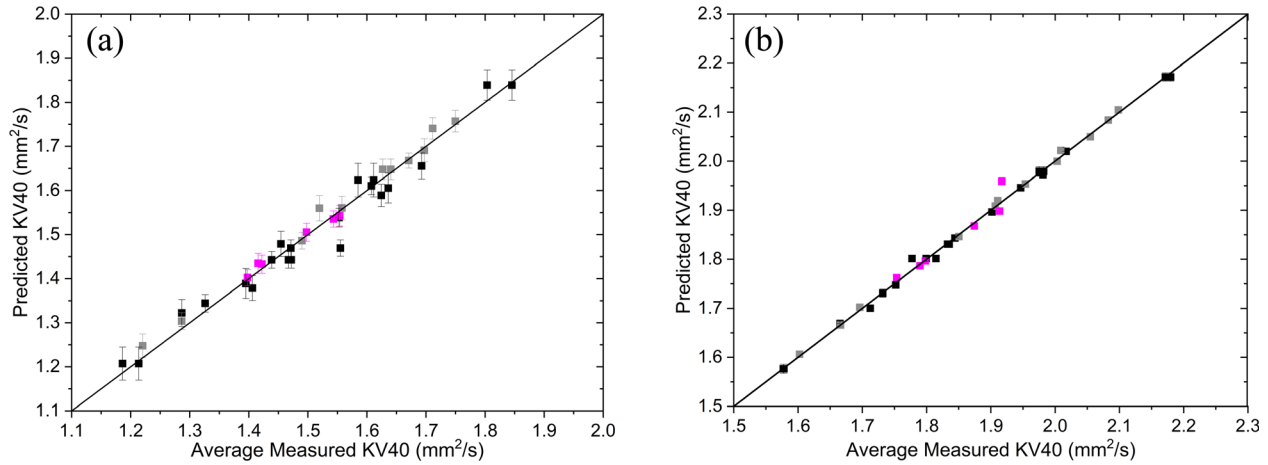

Fig. 9 Parity plots of the KV40 quadratic models generated by MODDE for (a) butyl-based blends, (b) pentyl-based blends. Black squares: MODDE generated blends, grey squares: additional blends added to increase coverage, and magenta squares: blends used to test the models.

conducting a sensitivity analysis perturbing different liquid properties. A smaller Sauter mean diameter indicates that smaller fuel droplets would form, improving the vaporisation of the fuel. The smaller droplets could have a positive impact on the combustion and, ultimately, the engine performance and emissions. However, a large reduction in the KV40 could affect the fuel injection causing fuel leakage, reducing the power output and increasing HC emissions from unburnt fuel.[77] For the pentyl-based biofuel blends, the viscosity limits of EN 590 and BS 2869 were satisfied by blends consisting of ≥75 vol% *n*PL, ≥5 vol% DNPE, and ≤20 vol% *n*PeOH.[12] Due to the higher viscosities compared to the butyl-based blends, a wider range of compositions of the pentyl-based blends would be suitable to blend with diesel whilst keeping the fuel blend compliant with viscosity limits.

Quadratic models were found to be the most suitable for predicting KV40s of the butyl and pentyl-based blends with R^2 values of 0.975 and 0.998, respectively (Fig. 9). For the butyl-based blends, all model terms were statistically significant except for the $DNBE^2$ term with a *p*-value of 0.25. However, due to the hierarchical nature of the fit, the $DNBE^2$ term is retained to preserve overall accuracy. For the pentyl-based blends, all model terms are statistically significant with *p*-values <0.05 (see S4.1 and S4.2†). The butyl and pentyl-based blends KV40 predictions have an AARD% from the measured value of 1.20% and 0.26%, respectively, indicating the quadratic equations can accurately model the KV40 for the three-component blends.

Blend boundaries for the three-component blends

MODDE was used to determine blend boundaries where different three-component blend compositions meet the limits for the three physical properties tested. There were no compliant blends that met the flash point, density, and KV40 limits of EN 590, BS 2869, or EN 14214 at the same time for any

Table 3 Room temperature miscibility limits for the ethyl-based blends with ULSD

Fraction of ULSD (vol%)	Fraction of total biofuel blend (vol%)	EL miscible fractions (vol%)	EtOH miscible fractions (vol%)	DEE miscible fraction (vol%)
20	80	50–75	5–20	20–45
30	70	50–75	5–20	20–45
50	50	50–75	5–20	20–45
75	25	50–75	5–20	20–45
90	10	50–90	5–20	5–45
95	5	50–90	5–20	5–45

Table 4 3 °C miscibility limits for the ethyl-based blends with ULSD

Fraction of ULSD (vol%)	Fraction of total biofuel blend (vol%)	EL miscible fractions (vol%)	EtOH miscible fractions (vol%)	DEE miscible fraction (vol%)
20	80	50–75	5–20	20–45
30	70	50–75	5–20	20–45
50	50	50–75	5–20	20–45
75	25	50–75	5–20	20–45
90	10	50–90	5–20	5–45
95	5	50–90	5–20	5–45

Table 5 Room temperature miscibility limits for the butyl-based blends with ULSD

Fraction of ULSD (vol%)	Fraction of total biofuel blend (vol%)	*n*BL miscible fractions (vol%)	*n*BuOH miscible fractions (vol%)	DNBE miscible fraction (vol%)
20	80	50–90	5–45	5–45
30	70	50–90	5–45	5–45
50	50	50–90	5–45	5–45
75	25	50–90	5–45	5–45
90	10	50–90	5–45	5–45
95	5	50–90	5–45	5–45

Table 6 3 °C miscibility limits for the butyl-based blends with ULSD

Fraction of ULSD (vol%)	Fraction of total biofuel blend (vol%)	*n*BL miscible fractions (vol%)	*n*BuOH miscible fractions (vol%)	DNBE miscible fraction (vol%)
20	80	50–75	5–40	10–45
30	70	50–80	5–45	5–45
50	50	50–90	5–45	5– 45
75	25	50–90	5–45	5–45
90	10	50–90	5–45	5–45
95	5	50–90	5–45	5–45

of the ethyl and butyl-based blends.[11,13] The blend of 90 vol% *n*BL/5 vol% DNBE/5 vol% *n*BuOH has a flash point that meets the 55 °C minimum of EN 590 and BS 2869, but it does not meet the density limits of EN 590 or EN 14214 and the KV40 limits of all three standards.[11–13] For the pentyl-based blends, a compliant set of blends could be found when using the BS 2869 properties limits, giving boundaries of ≥75 vol% *n*PL, ≥5 vol% DNPE, and ≤20 vol% *n*PeOH. The functionality of MODDE made determining these blend boundaries more time effective and reliable since it used the predictive models generated from the experimentally measured physical properties. The results indicate that the production of the blends needs to ensure a low content of the starting alcohol, which, during the production process, could be recycled for further biomass alcoholysis, improving economic favourability.[10,78] To be able to utilise higher volumetric blends of three-component biofuel compositions, such as those tested here within commercial fuels, it may require changes to standard limits for physical properties. However, the flash point limit carries implications for safe fuel handling and storage, so lowering this

limit would be unlikely and inadvisable. Since the density limits of biodiesel and off-road diesel are higher, the shift towards higher densities may be more feasible, as the aromatic content of the fuel would inherently reduce.

Blends with diesel

When the ethyl, butyl, and pentyl-based three-component mixtures were blended with ULSD, there were different limitations for each of the three-component biofuel blends. Most of the ethyl-based blends were immiscible with diesel, and the miscible blends had significant fractions of DEE, resulting in blends that could not have their flash points or KV40s tested. A limiting factor for utilising *n*PL is that the longer chain alcohol results in lower yields of alkyl levulinate during biomass alcoholysis.[31–34] Bio-derived *n*-pentanol is also scarce, and its production routes are still in development.[79] This makes the alcoholysis using *n*-pentanol less attractive compared to using ethanol or *n*-butanol, especially if fossil-derived *n*-pentanol was used. Hence, with the limitations of the ethyl and pentyl-based blends, butyl-based blends appear to be the most promising candidates for further investigation on blending behaviour with diesel. Therefore, they were investigated to determine the miscibility of the blends with ULSD and the resulting changes in physical properties at different volume fractions. The miscibility of the ethyl and butyl-based three-component blends with ULSD at room temperature and 3 °C are summarised in Tables 3–6. Due to the duration of the storage tests, the miscibility of the ethyl-based blends with diesel were conducted alongside the physical properties testing, and hence their results are presented here.

The room temperature storage of the ethyl-based blends with ULSD demonstrated that there needed to be at least 20 vol% of DEE but no more than 25 vol% of ethanol in the three-component blend to avoid separation when blended at significant fractions into ULSD. The separation of diesel/biofuel blends without these compositions of the ethyl-based biofuel blend occurred within minutes of blending. At room temperature, all the butyl-based blends with ULSD were miscible, regardless of the ULSD fraction. Due to the complex nature of miscibility and its dependence on intermolecular interactions between all of the components, predictive models would require extensive development and hence have not been attempted in this work. The complexity further increases when there are mixtures of hydrocarbons and oxygenated components, such as those investigated in this study. A model for a multi-component blend with a base fuel could become extremely complex due to all the possible interactions and intermolecular forces. This is highlighted by the need for high DEE fractions to ensure EL and EtOH also remained miscible with the ULSD, as shown in Table 3.

When blended with low fractions of ULSD and stored at 3 °C, both the ethyl and butyl-based blends formed solid white suspensions, with an example shown in Fig. 10. For the ethyl-based blends, this occurred regardless of the EL fraction, whereas, for butyl-based blends, this suspension only formed with a biofuel fraction ≥70 vol%. When the *n*BL fraction was >75 vol%, the suspension would form regardless of the *n*BuOH and DNBE fractions. If the BuOH fraction was greater than the DNBE fraction, then this suspension formed with lower *n*BL fractions, as it formed for the blend D20Bu80-50 : 5 : 45. The formation of the suspension indicates that these fuel blends would not be suitable for utilisation in cold temperatures, as these deposits may pose a blockage risk for fuel pumps and filters. The suspensions formed would melt within minutes of the test tubes being at room temperature. Hence, it was not possible to isolate these solids for further analysis to determine their composition.

Fig. 10 Example of the white suspensions formed when the some fuel blends are stored at 3 °C. Fuel blend above is D20Bu80 – 85 : 15 : 5.

Butyl-based blends with diesel

After identifying that, the butyl-based blends were the most suitable biofuel mixture to blend with diesel, the flash points, KV40s, and densities at 15 °C, when blended at different volume fractions, were measured. Tables of the data presented in Fig. 11 can be seen in S5.4.†

The flash points of the butyl-based blends with ULSD ranged between 38–57 °C for the different ULSD volume fractions. The blends with higher biofuel fractions had a greater reduction from the 65 °C flash point of the ULSD. As the *n*BL fraction within the three-component blend decreased, the flash point decreased when the diesel fraction was constant. This reduction was expected as the flash point of the pure butyl-based three-component blend reduced as the *n*BL fraction decreased. When blended with ULSD, the butyl-based biofuel blends with higher *n*-butanol fractions have lower flash points, despite *n*-butanol having a higher flash point than DNBE, as shown by the crossover at higher diesel fractions with the higher DNBE fraction blends in Fig. 11a. This crossover could be due to more favourable molecular interactions between DNBE and the hydrocarbons in ULSD since DNBE is effectively an eight-carbon long chain, albeit with oxygen in the centre, which is approaching the chain length of molecules typically found in ULSD.[25–30] In contrast, *n*-butanol has a four-carbon long chain and is more polar than DNBE. This leads to less favourable

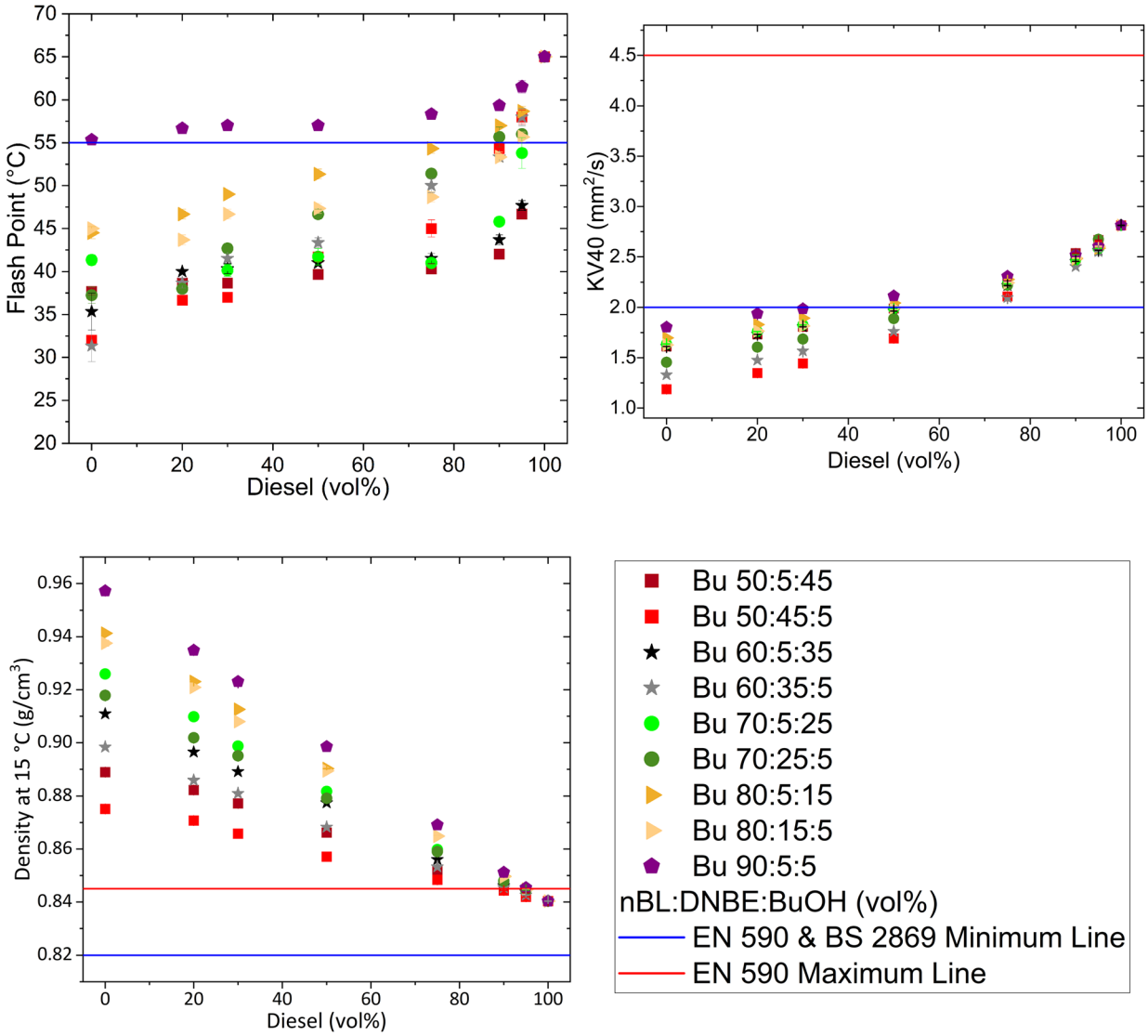

Fig. 11 (a) Flash point. (b) Kinematic viscosity at 40 °C. (c) Density at 15 °C for butyl three component blends with diesel. (d) Legend for all three plots. The blue lines indicate any EN 590 and BS 2869 minimums and the red lines indicate EN 590 maximums. EN 590 and BS 2869 compliant regions are indicated for each property.

molecular interactions with ULSD, causing the *n*-butanol to readily evaporate, producing a flammable vapour.[80] There were a small number of blends that had a flash point >55 °C.[12,13] These contained >70 vol% *n*BL, DNBE volume fractions greater than those of *n*BuOH, and >75% ULSD by volume. However, these flash points ranged between 55–62 °C and may not be sufficiently above the 55 °C limits of EN 590 and BS 2869 since the flash points of different commercial diesel are usually around 65 °C to allow sufficient margin to account for experimental errors that can occur with flash point testing.[12,13] The increase in flash point with diesel fraction was non-linear, having two distinct regions: high diesel fractions where the biofuel content decreases the flash point rapidly, and low diesel fractions where the flash point is close to that of the three-component biofuel blend.

The KV40 of the butyl-based blends with diesel depends upon the KV40 of the diesel used. For the diesel used in this study, up to 25 vol% of the butyl-based biofuel blends could be blended with the ULSD and produce compliant blends, as seen in Fig. 11b, since the KV40 did not drop below 2.0 $mm^2\ s^{-1}$.[12,13] If the viscosity of ULSD was higher, then higher fractions of the butyl-based blends could be added, and the fuel would remain compliant and within the viscosity limits. The lower viscosity of the fuel blends could lead to reduced lubrication in the fuel injection system.[17] The butyl-based blends that had lower viscosities (low *n*BL fractions with high DNBE fractions) caused a greater reduction in the KV40 for any given fraction of ULSD. The KV40 of the blends with ULSD had a non-linear dependence on the volume fraction of the ULSD fraction, albeit less pronounced than that which the flash points displayed. The

gradient of the change in KV40 is much greater when the fraction of ULSD is above 75 vol% than when the ULSD fraction is less than 75 vol%.

As previously discussed, the density of butyl-based blends was over the maximum limits specified in the EN 590 standard.[12] The addition of more than 5 vol% of any butyl-based blend to diesel produced biofuel/diesel blends that exceeded this maximum, as shown in Fig. 11c. Density increased linearly with increasing biofuel blend fraction when blending with ULSD, with the greater increases in the density being from the butyl-based blends with the higher density (those with the higher *n*BL fractions). If the ULSD used had a lower density, a higher fraction of the biofuel blends could be added and still meet the EN 590 limits.[12]

As the narrow EN 590 density limits inhibit large fractions of the butyl-based blends being added to diesel, compatibility with the BS 2869 density limits was also investigated. For 10 vol% biofuel in ULSD, the butyl-based blends could consist of ≥60 vol% *n*BL, ≤35 vol% DNBE, and ≤10 vol% *n*BuOH and remain compliant with BS 2869.[13] For 25 vol% biofuel the butyl-based blends could consist of ≥80 vol% *n*BL, ≤15 vol% DNBE, and ≤5 vol% *n*BuOH and remain within the limits. The low fractions of *n*BuOH in the compliant blends was due to its impact on the reduction in flash point of the blends with diesel.

Discussion of future fuel standards

As previously mentioned, EN 590 and BS 2869 do not allow the addition of oxygenated advanced biofuel components.[12] However, since RED II requires at least 3.5% of the energy in the transport sector to be sourced from advanced biofuels by 2030, the relaxation or modification of fuel standards may be necessary to facilitate the utilisation of oxygenated advanced biofuels from cheaper, less carbon-intensive fuel production methods.[6] The use of oxygenated fuels could potentially have benefits for engine emissions, but could also reduce the energy density of the fuel. However, this has not inhibited the use of oxygenated fuels within gasoline blends which now contain bioethanol. The use of oxygenated advanced biofuels other than ethanol is not allowed in the low-carbon fuel standards adopted by several states in the United States of America or the EU. However, in the EU, there are targets for the increased use of advanced biofuels, but Annex III of RED II does not list alkyl levulinates and dialkyl ethers as potential biofuel options, nor are any oxygenated fuels other than FAME allowed to be blended with diesel.[6,11–13] The utilisation of oxygenated advanced biofuel blends that meet physical, chemical, and combustion property limits in existing fuel standards will be inhibited until a wider range of oxygenated species are permitted. Therefore, a global change to the fuel standards is required to enable the use of oxygenated fuels that could contribute towards the low-carbon fuel options for the decarbonisation targets to be more easily met.[81–83] In this study we have shown that the selected properties can be met by certain blends, but there are additional physical property limits that must be met for a fuel to be certified. These include oxidative stability, copper corrosion, and lubricity.[12,13] A review of the density limits could also be useful, as in EN 590 they are set as an additional control measure to limit the PAH content of the fuel. This measure has likely contributed to the control of particulate emissions. However, many studies have shown that particulate emissions reduce when oxygenated biofuels are blended with diesel, even when density limits are exceeded.[10,15,78] Therefore, if the engine performance is maintained, or improved, and emissions limits can be met upon utilisation of fuel blends that exceed the current density limits, then the maximum density limits could potentially be relaxed. To make progress in the utilisation of these advanced biofuel blends, there either needs to be amendments to existing fuel standards or the development of separate fuel standards for oxygenated advanced biofuels, in a similar manner to the EN 14214 standard for biodiesels.[11]

Conclusions

In this study, the flash point, KV40, and density at 15 °C were tested, where applicable, for model three-component biofuel blends with increasing carbon chain lengths, with and without diesel. The DoE methodology enabled the production of simple and accurate predictive models for the selected physical properties of the three-component blends. Therefore, it is likely, that this methodology could be used to develop predictive models for other physical properties. It also allowed a more efficient testing regime to be used. The influence of the carbon chain length could be observed from the testing conducted, not only on the physical properties, but also on the biofuel miscibility with ULSD. The immiscibility of the ethyl-based blends with diesel when the ethanol fraction was higher than the DEE fraction highlights that the presence of high quantities of the polar short carbon chain length alcohol would cause separation, whereas this did not occur for the butyl-based blends.

Increasing carbon chain length increased the flash point and KV40 of the three-component blends. As the carbon chain length increased, the density of the three-component blends remained similar for the blends with <65 vol% alkyl levulinate. In contrast, the blends with >70 vol% of the alkyl levulinate had lower densities, as the carbon chain length increased due to the reduction in the density of the alkyl levulinate, even though the density of the alcohol and the dialkyl ether increased with carbon chain length. The dialkyl ethers and alkyl levulinates became closer to the chain lengths of components typically found in diesel as the chain length of the starting alcohol increased.

Predicting the flash points and KV40s of the pure biofuel blends investigated in this study, required nonlinear blending rules that were able to account for the interaction effects observed. Blends with diesel would require nonlinear blending rules to be generated, given the nature of the behaviours observed in Fig. 11a and b. Flash points and KV40 of the butyl and pentyl-based blends could be accurately predicted using quadratic models with high R^2 values and an AARD% of less than 5% between measured and predicted values for each of the properties. The models had statistically significant coefficients for second-order interaction terms. The density of the blends could be modelled using a linear model as developed here using MODDE, or with the commonly used linear blending law. Whilst the developed models are limited to the blends tested

here, the DoE methodology makes the model production an efficient process that may be applied to other fuel blends.

Flash points of the butyl and pentyl-based three-component blends are highly dependent upon the fraction of the component with the lowest flash point, DNBE and *n*PeOH, respectively, with higher fractions of these components giving a greater reduction. However, when the butyl-based blends were blended with diesel, there was a greater reduction in flash points for blends with high alcohol fractions. For example, for the blends of 75 vol% ULSD/25 vol% biofuel with 70 vol% *n*BL, there was a reduction of 25% relative to diesel for the blend which contained 25 vol% *n*BuOH compared to that of the blend with 5 vol% *n*BuOH. *n*BuOH has the shortest carbon chain length of the butyl-based three components and is the most polar component, resulting in reduced favourable molecular interactions with ULSD. However, these results indicate DNBE has favourable intermolecular interactions with the compounds in ULSD. This was evident since *n*BuOH has a higher flash point than DNBE. Removing *n*BuOH from the biofuel blend could increase the flash points of the blends with ULSD to over the limits in the fuel standards. Additionally, economically, it could be beneficial to remove or vastly reduce *n*BuOH within the product blend, as it could be recycled for further biomass alcoholysis.[10,64,78]

Existing fuel standard limits for the flash point and KV40 can be met with increasing carbon chain length in oxygenated blends, as shown in this study by increasing from C2 to C5 alcohols and their corresponding alkyl levulinates and ethers, whereas the density limits are difficult to meet, as the limits are very narrow. Since the alkyl levulinate is the largest fraction of the blends, the decreasing density with increasing carbon chain length will dictate if the limits of the fuel standards are met. The densities of these components are much greater than the current limits in EN 590 and EN 14214.[11,12] Therefore, to enable a wider range of oxygenated biofuel components to be utilised, density limits in existing fuel standards would need to be extended. Other changes to the existing fuel standards would also be required, such as allowing the addition of other non-FAME oxygenated bio-derived fuels for diesel blending, where they are shown to maintain or improve engine performance and emissions relative to diesel. This could facilitate meeting the RED II advanced biofuel and decarbonisation targets. In addition to meeting physical property limits, materials compatibility and suitability for engine use also need to be determined for such blends, and are currently being addressed in parallel work by the authors.

Author contributions

Scott Wiseman: investigation, data curation, formal analysis, investigation, writing – original draft. Christian A. Michelbach: writing – original draft, data curation. Hu Li: supervision, writing – review & editing. Alison S. Tomlin: supervision, writing – original draft.

Conflicts of interest

There are no conflicts of interest to declare.

Acknowledgements

This research is supported by UKRI EPSRC training grant, EP/L014912/1, regulated by the University of Leeds Centre for Doctoral Training in Bioenergy. Thanks to Dr Adrian Cunliffe and Karine Alves-Thorne in the University of Leeds, School of Chemical and Process Engineering's Analytical Laboratory for their training and support. Grateful thanks go to Dr Alastair Baker for securing the licenses of MODDE and for his training and support using the DoE methodology.

References

1 *2019 UK Greenhouse Gas Emissions, Final Figures*, London, Department for Business, Energy & Industrial Strategy and Office for National Statistics, 2021.
2 Department for Transport, *TSGB0301 (ENV0101): Petroleum consumption by transport mode and fuel type*, **https://www.gov.uk/**, accessed 27/01/2022, 2022.
3 International Energy Agency, *Global EV Outlook 2021*, 2021.
4 European Environment Agency, *EEA greenhouse gases – data viewer*, **https://www.eea.europa.eu/**, accessed 29/07/2022, 2022.
5 United States Environmental Protection Agency, *Inventory of U.S. Greenhouse Gas Emissions and Sinks: 1990-2019*, 2021.
6 The European Parliament and Council of the European Union, *Directive (EU) 2018/2001 of the European Parliament and of the Council of 11 December 2018 on the promotion of the use of energy from renewable sources*, **https://eur-lex.europa.eu**, accessed 29/10/2019, 2019.
7 I. Dimitriou, H. Goldingay and A. V. Bridgwater, *Renewable Sustainable Energy Rev.*, 2018, **88**, 160–175.
8 M. S. Howard, G. Issayev, N. Naser, S. M. Sarathy, A. Farooq and S. Dooley, *Sustainable Energy Fuels*, 2019, **3**, 409–421.
9 T. Flannelly, S. Dooley and J. J. Leahy, *Energy Fuels*, 2015, **29**, 7554–7565.
10 C. Antonetti, S. Gori, D. Licursi, G. Pasini, S. Frigo, M. Lopez, J. C. Parajo and A. M. R. Galletti, *Catalysts*, 2020, **10**, 509.
11 British Standards Institution, *Fatty Acid Methyl Esters (FAME) for Use in Diesel Engines and Heating Applications*. Requirements and test methods, Milton Keynes, 2019.
12 British Standards Institution, *Automotive Fuels – Diesel – Requirements and Test Methods*, Milton Keynes, 2022.
13 British Standards Institution, *Fuel Oils for Agricultural, Domestic and Industrial Engines and Boilers*, Milton Keynes, 2022.
14 *Using Rebated Fuels in Vehicles and Machines (Excise Notice 75) from 1 April 2022*, London, UK, HM Revenue & Customs, 2022.
15 E. Christensen, A. Williams, S. Paul, S. Burton and R. L. McCormick, *Energy Fuels*, 2011, **25**, 5422–5428.
16 Worldwide Fuel Charter Committee, *Worldwide Fuel Charter 2019 – Gasoline and Diesel Fuel*, 2019.
17 M. Lapuerta, J. Rodríguez-Fernández, D. Fernández-Rodríguez and R. Patiño-Camino, *Fuel*, 2017, **199**, 332–338.
18 D. M. Korres, G. Anastopoulos, E. Lois, A. Alexandridis, H. Sarimveis and G. Bafas, *Fuel*, 2002, **81**, 1243–1250.

19 M. Lapuerta, R. García-Contreras, J. Campos-Fernández and M. P. Dorado, *Energy Fuels*, 2010, **24**, 4497–4502.
20 L. Y. Phoon, A. A. Mustaffa, H. Hashim and R. Mat, *Ind. Eng. Chem. Res.*, 2014, **53**, 12553–12565.
21 H.-J. Liaw, Y.-H. Lee, C.-L. Tang, H.-H. Hsu and J.-H. Liu, *J. Loss Prev. Process Ind.*, 2002, **15**, 429–438.
22 E. Torres-Jimenez, M. S. Jerman, A. Gregorc, I. Lisec, M. P. Dorado and B. Kegl, *Fuel*, 2011, **90**, 795–802.
23 D. Kim, J. Martz and A. Violi, *Fuel*, 2016, **180**, 481–496.
24 P. Hellier, M. Talibi, A. Eveleigh and N. Ladommatos, *Proc. Inst. Mech. Eng., Part D*, 2018, **232**, 90–105.
25 F. L. Dryer, *Proc. Combust. Inst.*, 2015, **35**, 117–144.
26 C. J. Mueller, W. J. Cannella, J. T. Bays, T. J. Bruno, K. DeFabio, H. D. Dettman, R. M. Gieleciak, M. L. Huber, C.-B. Kweon, S. S. McConnell, W. J. Pitz and M. A. Ratcliff, *Energy Fuels*, 2016, **30**, 1445–1461.
27 Y. Wu, *Doctor of Philosophy*, University of Leeds, 2019.
28 Y. Wu, H. Li and G. Andrews, *SAE Technical Paper*, 2020-01-2059, DOI: **10.4271/2020-01-2059**.
29 J. Zhu, D. Zhou, L. Yu, Y. Qian and X. Lu, *Fuel*, 2022, **313**, 122711.
30 Y. Zhu, M. Jia, B. Niu, J. Tian, H. Li and J. Fan, *Fuel*, 2022, **310**, 122424.
31 S. Zhu, J. Guo, X. Wang, J. Wang and W. Fan, *ChemSusChem*, 2017, **10**, 2547–2559.
32 K. Alamgir Ahmad, M. Haider Siddiqui, K. K. Pant, K. D. P. Nigam, N. P. Shetti, T. M. Aminabhavi and E. Ahmad, *Chem. Eng. J.*, 2022, **447**, 137550.
33 A. M. Raspolli Galletti, C. Antonetti, S. Fulignati and D. Licursi, *Catalysts*, 2020, **10**, 1221.
34 A. Démolis, N. Essayem and F. Rataboul, *ACS Sustain. Chem. Eng.*, 2014, **2**, 1338–1352.
35 Y.-X. Huo, K. M. Cho, J. G. L. Rivera, E. Monte, C. R. Shen, Y. Yan and J. C. Liao, *Nat. Biotechnol.*, 2011, **29**, 346–351.
36 R. Andersson, M. Boutonnet and S. Järås, *Fuel*, 2014, **115**, 544–550.
37 C. Jin, M. Yao, H. Liu, C.-f. F. Lee and J. Ji, *Renewable Sustainable Energy Rev.*, 2011, **15**, 4080–4106.
38 B. O. Abo, M. Gao, Y. Wang, C. Wu, Q. Wang and H. Ma, *Environ. Sci. Pollut. Res.*, 2019, **26**, 20164–20182.
39 H. A. Schuette and M. A. Cowley, *J. Am. Chem. Soc.*, 1931, **53**, 3485–3489.
40 *VWR, Ethanol: MSDS No. 7669152*, **https://uk.vwr.com/**, accessed 21/11/2019, 2019.
41 *Honeywell, 1-Butanol: MSDS No. 000000020528*, **https://www.honeywellmsds.com/**, accessed 12/12/2019, 2019.
42 *Thermo Fisher Scientific, Di-n-butyl ether; MSDS No. ACR14969*, **https://www.fishersci.co.uk/**, accessed 16/10/2019, 2019.
43 *Sigma Aldrich, Diethyl ether; MSDS No. 296082*, **https://www.sigmaaldrich.com/**, accessed 21/06/2019, 2019.
44 *Sigma Aldrich, Ethyl Levulinate; MSDS No. 122629*, **https://www.sigmaaldrich.com/**, accessed 21/06/2019, 2019.
45 *Thermo Fisher Scientific, n-Butyl levulinate; MSDS No. ALFAAG59274*, **https://www.alfa.com/**, accessed 16/10/2019, 2019.
46 *Sigma Aldrich, 1-Pentanol; MSDS No. 76929*, **https://www.sigmaaldrich.com/**, accessed 21/07/2021, 2021.
47 *Sigma Aldrich, Di-n-amyl ether for synthesis; MSDS No. 8.20964*, **https://www.sigmaaldrich.com/**, accessed 21/07/2021, 2021.
48 *Chemspace, Pentyl 4-Oxopentanoate; MSDS No. CSC000076155*, 2021.
49 H. Kuszewski, *Energy Fuels*, 2018, **32**, 11619–11631.
50 M. Hristova and D. Damgaliev, *Cent. Eur. J. Chem.*, 2013, **11**, 388–393.
51 L. Catoire, S. Paulmier and V. Naudet, *Process Saf. Prog.*, 2006, **25**, 33–39.
52 E. A. Hernández, G. Sánchez-Reyna and J. Ancheyta, *Fuel*, 2021, **283**, 118941.
53 M. Gülüm and A. Bilgin, *Fuel*, 2017, **199**, 567–577.
54 M. J. Pratas, S. V. D. Freitas, M. B. Oliveira, S. C. Monteiro, Á. S. Lima and J. A. P. Coutinho, *Energy Fuels*, 2011, **25**, 2333–2340.
55 E. Alptekin and M. Canakci, *Renewable Energy*, 2008, **33**, 2623–2630.
56 I. Barabás, *Fuel*, 2013, **109**, 563–574.
57 L. Catoire, S. Paulmier and V. Naudet, *J. Phys. Chem. Ref. Data*, 2006, **35**, 9–14.
58 J. Lohmann, R. Joh and J. Gmehling, *Ind. Eng. Chem. Res.*, 2001, **40**, 957–964.
59 J. Gmehling, R. Wittig, J. Lohmann and R. Joh, *Ind. Eng. Chem. Res.*, 2002, **41**, 1678–1688.
60 A. Jakob, H. Grensemann, J. Lohmann and J. Gmehling, *Ind. Eng. Chem. Res.*, 2006, **45**, 7924–7933.
61 L. Y. Phoon, H. Hashim, R. Mat and A. A. Mustaffa, *J. Eng. Sci. Technol.*, 2015, **10**, 110–119.
62 H.-J. Liaw, C.-L. Tang and J.-S. Lai, *Combust. Flame*, 2004, **138**, 308–319.
63 L. Grunberg and A. H. Nissan, *Nature*, 1949, **164**, 799–800.
64 J. F. Leal Silva, R. Grekin, A. P. Mariano and R. Maciel Filho, *Energy Technol.*, 2018, **6**, 613–639.
65 Sartorius Stedim Data Analytics, *User Guide to MODDE. Version 12*, **https://landing.umetrics.com/**, accessed 30/1/2020, 2020.
66 W. DuMouchel and B. Jones, *Technometrics*, 1994, **36**, 37–47.
67 R. D. Cook and C. J. Nachtsheim, *Technometrics*, 1980, **22**, 315–324.
68 L. Eriksson, *D-optimal design – what it is and when to use it*, **https://www.youtube.com/**, accessed 17/04/2020, 2020.
69 M. E. Johnson and C. J. Nachtsheim, *Technometrics*, 1983, **25**, 271–277.
70 E. Walter and L. Pronzato, *Automatica*, 1990, **26**, 195–213.
71 British Standards Institution, *Determination of Flash No Flash and Flash Point — Rapid Equilibrium Closed Cup Method,* Milton Keynes, 2015.
72 British Standards Institution, *Petroleum Products and Related Products. Determination of Kinematic Viscosity*, Method by Stabinger type viscosimeter, Milton Keynes, 2016.
73 British Standards Institution, *Crude Petroleum and Liquid or Solid Petroleum Products – Determination of Density or Relative Density – Capillary-Stoppered Pyknometer and Graduated Bicapillary Pyknometer Methods,* Milton Keynes, 2014.

74 British Standards Institution, *Methods of Test for Petroleum and its Products. Crude Petroleum and Petroleum Products. Determination of Density*, Oscillating U-tube method, Milton Keynes, 1996.
75 H. Liu, J. Ma, F. Dong, Y. Yang, X. Liu, G. Ma, Z. Zheng and M. Yao, *Energy Convers. Manage.*, 2018, **171**, 1787–1800.
76 European Parliament, *Regulation (EC) No 1272/2008 of the European Parliament and of the Council of 16 December 2008 on classification, labelling and packaging of substances and mixtures, amending and repealing Directives 67/548/EEC and 1999/45/EC, and amending Regulation (EC) No 1907/2006*, **http://eur-lex.europa.eu/**, accessed 10/03/2022, 2022.
77 G. N. Singh and R. S. Bharj, *Sustainable Chem. Pharm.*, 2019, **12**, 100130.
78 S. Frigo, G. Pasini, G. Caposciutti, M. Antonelli, A. M. R. Galletti, S. Gori, R. Costi and L. Arnone, *Fuel*, 2021, **297**, 120742.
79 A. F. Cann and J. C. Liao, *Appl. Microbiol. Biotechnol.*, 2010, **85**, 893–899.
80 M. Lapuerta, J. Rodríguez-Fernandez, R. García-Contreras and M. Bogarra, *Fuel*, 2015, **139**, 171–179.
81 G. E. Lade and C. Y. C. Lin Lawell, *Res. Transp. Econ.*, 2015, **52**, 91–99.
82 S. Huseynov and M. A. Palma, *PLoS One*, 2018, **13**, e0203167.
83 J. Witcover and C. Murphy, *Transp. Res. Rec.*, 2021, **2675**, 367–378.

